

ORIGINAL PAPER

M. O. Garcia · K. H. Rubin · M. D. Norman
J. M. Rhodes · D. W. Graham · D. W. Muenow
K. Spencer

Petrology and geochronology of basalt breccia from the 1996 earthquake swarm of Loihi seamount, Hawaii: magmatic history of its 1996 eruption

Received: 21 August 1997 / Accepted: 15 February 1998

Abstract Samples of basalt were collected during the Rapid Response cruise to Loihi seamount from a breccia that was probably created by the July to August 1996 Loihi earthquake swarm, the largest swarm ever recorded from a Hawaiian volcano. ^{210}Po – ^{210}Pb dating of two fresh lava blocks from this breccia indicates that they were erupted during the first half of 1996, making this the first documented historical eruption of Loihi. Sonobuoys deployed during the August 1996 cruise recorded popping noises north of the breccia site, indicating that the eruption may have been continuing during the swarm. All of the breccia lava fragments are tholeiitic, like the vast majority of Loihi's most recent lavas. Reverse zoning at the rim of clinopyroxene phenocrysts, and the presence of two chemically distinct olivine phenocryst populations, indicate that the magma for the lavas was mixed just prior to eruption. The trace element geochemistry of these lavas indicates there has been a reversal in Loihi's temporal geochemical trend. Although the new Loihi lavas are similar isotopically and geochemically to recent Kilauea lavas and the mantle conduits for these two volcanoes appear to converge

at depth, distinct trace element ratios for their recent lavas preclude common parental magmas for these two active volcanoes. The mineralogy of Loihi's recent tholeiitic lavas signify that they crystallized at moderate depths (~8–9 km) within the volcano, which is approximately 1 km below the hypocenters for earthquakes from the 1996 swarm. Taken together, the petrological and seismic evidence indicates that Loihi's current magma chamber is considerably deeper than the shallow magma chamber (~3–4 km) in the adjoining active shield volcanoes.

Key words Hawaii · Loihi · Magmatic processes · Submarine volcanism · Petrology · Geochronology · Lava geochemistry

Introduction

The largest swarm of earthquakes ever observed at any Hawaiian volcano occurred at Loihi seamount during late July and early August of 1996. To investigate this event, a marine expedition was dispatched to Loihi in early August on the R/V Kaimikai-O-Kanaloa (K-O-K). The volcanological, tectonic, hydrothermal, and biological activities associated with this event were investigated during the Rapid Response (RR) cruise using Seabeam surveys of the entire volcano, numerous water sampling deployments, sonobuoys, an ocean bottom seismometer (OBS), and two PISCES V submersible dives. The most obvious result of the earthquake activity was the formation of a new large summit pit crater (Loihi Science Team 1997). Intense hydrothermal plumes were detected in the surrounding water column, and fresh glassy rocks were recovered, indicating that an eruption may have accompanied the earthquake swarm.

In this paper, we report the results from petrological, geochemical, and geochronological studies of lavas collected during two submersible dives from a new breccia deposit that was created during the earthquake swarm. The breccia is not present near the new pit crater

Editorial responsibility: D. Swanson

Michael O. Garcia (✉) · Ken H. Rubin · Khalil Spencer
Department of Geology and Geophysics, Hawaii Center for
Volcanology, University of Hawaii, Honolulu, Hawaii 96822,
USA

Marc D. Norman
Key Centre for the Geochemical Evolution and Metallogeny of
the Continents (GEMOC), School of Earth Sciences, Macquarie
University, North Ryde, NSW 2109 Australia

J. Michael Rhodes
Department of Geosciences, University of Massachusetts,
Amherst, MA 01003, USA

David W. Graham
College of Oceanic and Atmospheric Sciences, Oregon State
University, Corvallis, OR 97331–5503, USA

David W. Muenow
Department of Chemistry, University of Hawaii, Honolulu,
Hawaii 96822, USA

er, which appears to have collapsed without ejecting debris. Our results show that two glassy rocks from this breccia, the freshest ever recovered from Loihi, were erupted during the first half of 1996. This is the first documented case of a historical eruption of Loihi, although ten previous earthquake swarms have been recorded from the volcano (Bryan and Cooper 1995). Although the eruption dates for these two lavas predate the major earthquake swarm, sonobuoys deployed near the end of the swarm recorded popping noises that may have been related to an ongoing submarine Loihi eruption (Loihi Science Team 1997). Insufficient data are available to determine whether there was more than one eruption at Loihi in 1996. All of the new lavas are tholeiitic and are remarkably similar in composition to other Loihi summit tholeiites (e.g., Garcia et al. 1995). The rocks from the breccia display mineralogical evidence of magma mixing just prior to their eruption. We hypothesize that magma mixing may have triggered the 1996 eruption.

Petrological and seismic evidence indicate that the magma for this eruption probably ascended from a moderate depth reservoir ($\sim 8\text{--}9\text{ km}$), which is deeper within the volcano than the crustal magma chamber in the other active Hawaiian volcanoes ($3\text{--}4\text{ km}$; Decker et al. 1983; Klein et al. 1987) but is shallower than a previous estimate for Loihi (16 km ; Clague 1988). Many of the younger tholeiitic lavas from the summit of the volcano have mineralogical evidence of storage in a moderate depth magma chamber. This evidence is absent in the older alkalic Loihi lavas. We propose that the formation of this moderate depth magma chamber is a relatively recent feature at Loihi ($< 10\text{--}20\text{ ka}$) and that it is related to the higher magma supply rates associated with Loihi's transition from alkalic to tholeiitic volcanism. The greater depth of Loihi's chamber may be related to the cooler thermal regime in this submarine volcano.

Geologic setting

Loihi seamount is the most southern and recent shield volcano formed by the Hawaiian hotspot (Moore et al. 1982). It is located $\sim 35\text{ km}$ south of the island of Hawaii and is built on the flanks of two other active Hawaiian shield volcanoes (Mauna Loa and Kilauea), which formed on $\sim 105\text{ Ma}$ Pacific Ocean crust (Epp 1984; Waggoner 1993). Loihi reaches a maximum thickness of $\sim 3.5\text{ km}$ (Garcia et al. 1995) and rises to $\sim 1000\text{ m}$ below sea level (Fornari et al. 1988). Lavas collected from a stratigraphic section on the deeply dissected east flank of the volcano (total stratigraphic thickness $\sim 500\text{ m}$) have yielded reliable K–Ar ages of 5 ± 4 to $102 \pm 13\text{ ka}$. These ages have been used to estimate the overall age of Loihi as 250 ka (Guillou et al. 1997).

Loihi has two rift zones that strike north and south–southeast, giving the seamount a pronounced el-

ongate shape; this led to it being given the Hawaiian name Loihi, “the long one” (Emery 1955). The rift zones connect to a summit platform at $\sim 1200\text{ m}$ water depth, which has two $\sim 300\text{-m}$ -deep pit craters on its east and west flanks (Fig. 1). A third, slightly smaller, pit crater was created on the southern margin of the

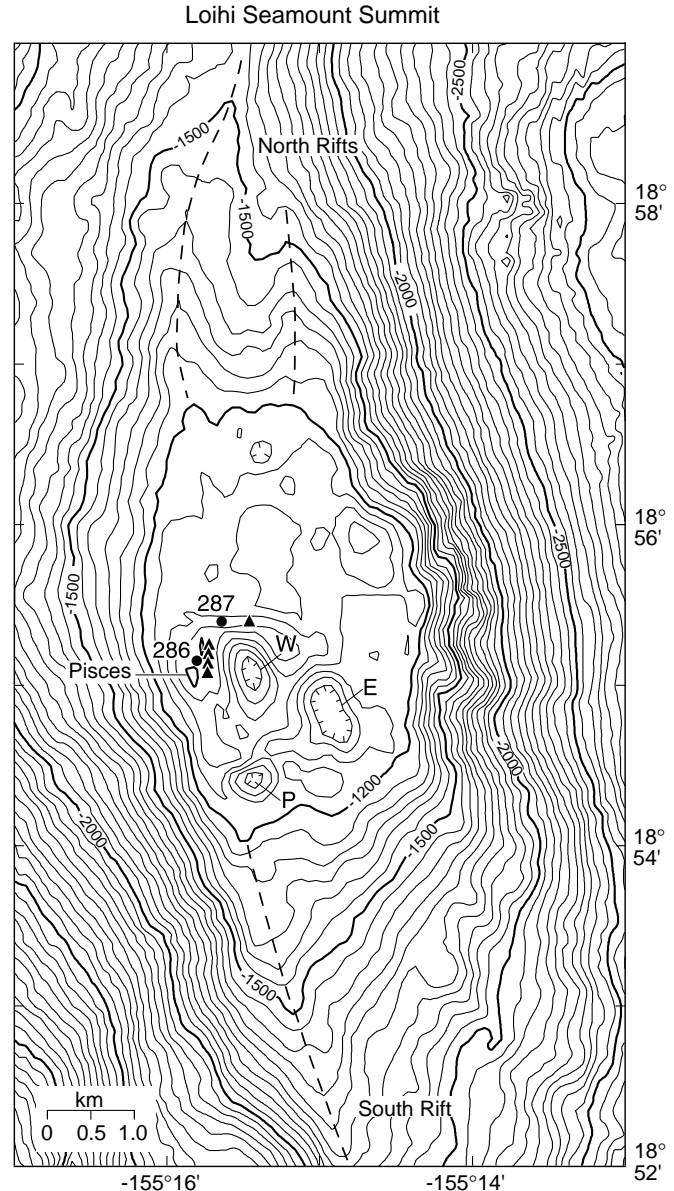


Fig. 1 Bathymetric map of the summit area of Loihi Volcano based on new Seabeam bathymetry collected after the 1996 earthquake swarm (compiled by J. R. Smith). Loihi's summit platform is defined by the 1200-m contour. The pit craters are labeled *W* (west), *E* (east), and *P* (Pele's). The new Pele's crater formed during the 1996 earthquake swarm (Loihi Science Team 1997). The locations where samples were collected during the two 1996 Pisces V dives (286 and 287) are shown by *solid circles*; *solid triangles* indicate the locations for the 1987 Alvin dive 1802 samples 20–25. Sample 1802-25 was collected just east of dive 287 sample site. Pisces Peak is the hill just south of the dive 286 sample site. It was bisected during the 1996 earthquake swarm (Loihi Science Team 1997). Rift zone axes are shown by *dashed lines*. The contour interval is 50 m

platform during the 1996 earthquake swarm (Loihi Science Team 1997). These pit craters are similar in diameter to some Kilauea pit craters but are ~100 m deeper.

Loihi was assumed to be a Cretaceous seamount unrelated to the Hawaiian hotspot (Moore and Fiske 1969) until it had major earthquake swarms in 1971–1972 and 1975 (Klein 1982). A marine expedition was organized in 1978 to investigate the source of the earthquakes. Dredging of the seamount recovered glassy basalt, confirming that the volcano was recently active, but no evidence was found for eruptions related to these earthquake swarms (Moore et al. 1982). Since 1975, eight earthquake swarms have occurred at Loihi (in 1984–1986, 1989–1991, 1993, 1995; Bryan and Cooper 1995). Earthquake swarms on active Hawaiian volcanoes are thought to be related to the movement of magma (Bryan and Cooper 1995), but no evidence of historic volcanic activity had been observed at Loihi prior to 1996, despite extensive camera and submersible surveys of the volcano. One problem with recognizing young lavas on Loihi is that they are covered with iron oxides shortly after eruption, so their potential youthfulness is obscured. Low-temperature (~30°C) hydrothermal venting has been reported in several areas around the summit of Loihi prior to 1996, especially at Pele's vents (e.g., Karl et al. 1988), the site where the new pit crater formed (Loihi Science Team 1997). Temperatures of ~200°C have been measured at vents in this new crater (T. Kerby, pers. commun.).

1996 Earthquake swarm and sampling summary

Between 16 July and 9 August 1996, over 4000 Loihi earthquakes were detected by the seismic network of the U. S. Geological Survey's Hawaiian Volcano Observatory (HVO). The initial phase of seismic activity continued for 2 days and was followed by 30 h of quiescence. Earthquake activity resumed and continued at a higher rate, averaging over 88 events per day for the next 10 days before slowing again. Hypocentral locations for these earthquakes are concentrated at depths 7–8 km below the volcano's summit (Caplan-Auerbach et al. 1997). Few shallow earthquakes (between 0 and 5 km) were located from this swarm, despite the formation of a new pit crater and a ring fracture with several meters of offset along the northern half of the summit platform (Loihi Science Team 1997).

Sonobuoys dropped from the K-O-K in early August during the RR cruise to listen for earthquakes and eruption sounds detected bangs, pops, and grinding noises with frequencies from tens to several hundred Hertz at three distinct locations on the northeast side of the summit, moving from south to north with time (Loihi Science Team 1997). Many of these sounds are similar to those recorded from Kilauea's shallow submarine pillow lava extrusion.

Two dives were made with the PISCES V submersible during the RR cruise to investigate the geological consequences of the earthquake swarm. The first dive (286) collected samples from the west flank of the summit platform just north of Pisces Peak, now the highest point on Loihi (Fig. 1). This area was visited in 1987 with the Alvin submersible (dive 1802; Garcia et al. 1993). In 1987 the Pisces Peak area was covered with pillow lavas with little or no coral growth but with a thin surface coating of iron oxides. After the 1996 earthquake swarm, this area was littered with broken weathered-rock debris. In the saddle just north of Pisces Peak, glassy rock fragments were found emerging from a deposit beneath the weathered rock debris. These glassy rocks are the freshest that have been recovered from Loihi. The glassy debris was found only in a localized area (30 × 50 m). The deposit seemed to form a thin veneer, ~30 cm thick, over older pillow lavas. The size of the larger glassy rock fragments increases toward the west pit crater where a new scarp with ~40 m of offset was observed. This scarp bisects Pisces Peak and was traced to the north for several hundred meters. During the second dive (287) on the northwest flank of the west pit, diving conditions were poor and only one weathered rock sample was collected from loose debris at the site (see Fig. 1).

Petrography and mineral chemistry

The lava samples collected during the Loihi RR cruise were photographed and described immediately following the cruise. These images were made available over the World Wide Web (<http://www.soest.hawaii.edu/GG/HCV/loihirocks.html>) with an invitation to scientists to request samples for study. This invitation remains open. The following is a compilation of the petrological and geochemical studies that have been completed on these rocks prior to August 1997.

The rocks collected from the Loihi 1996 breccia deposit range in length from 6 to 15 cm; all have glassy rims and appear to be fragments of pillow lava. Two of the samples have fresh glassy flow tops (286-1 and 286-6); the others appear to be slightly older because they have thin coatings of iron oxides on glass and fracture surfaces. The vesicularity of the samples varies from low (~5 vol.%) to moderate (15–20 vol.%). All of the lavas contain sparse (2 vol.%) to common (2–4 vol.%) olivine and clinopyroxene phenocrysts and microphenocrysts (Table 1) in a glassy matrix. The clinopyroxene phenocrysts are unusual for Hawaiian shield lavas, especially because some contain small (<0.05 mm across) inclusions of olivine near their core. The clinopyroxenes are euhedral and commonly sector zoned with concentric zoning near their rims. The olivines are mostly euhedral and undeformed, although some are resorbed and a few are weakly kink banded.

Olivine and clinopyroxene phenocrysts and microphenocrysts were analyzed by electron microprobe to

Table 1 Petrography and XRF whole-rock chemistry of lavas from the Loihi 1996 eruption breccia. The modes are based on 500 counts/sample except vesicularity, which was estimated.

Phenocrysts (ph) are >0.5 mm wide; microphenocrysts (mph) are 0.1–0.5 mm wide. Mg# is calculated assuming 10% oxidized iron. Total iron is reported as Fe₂O₃*

| Sample | 286-1 | 286-2 | 286-5 | 286-6 | 287-1 |
|--|-------|-------|-------|-------|-------|
| Whole-rock major elements (wt. %) | | | | | |
| SiO ₂ | 47.60 | 47.69 | 47.79 | 47.85 | 47.79 |
| TiO ₂ | 2.44 | 2.39 | 2.53 | 2.54 | 2.42 |
| Al ₂ O ₃ | 12.32 | 12.01 | 12.71 | 12.85 | 12.20 |
| Fe ₂ O ₃ * | 13.31 | 13.33 | 13.24 | 13.23 | 13.30 |
| MnO | 0.19 | 0.19 | 0.19 | 0.19 | 0.19 |
| MgO | 9.50 | 10.27 | 8.51 | 8.19 | 9.65 |
| CaO | 11.16 | 10.97 | 11.46 | 11.47 | 11.05 |
| Na ₂ O | 2.38 | 2.09 | 2.44 | 2.37 | 2.27 |
| K ₂ O | 0.42 | 0.39 | 0.47 | 0.45 | 0.41 |
| P ₂ O ₅ | 0.24 | 0.23 | 0.25 | 0.25 | 0.24 |
| Total | 99.57 | 99.55 | 99.59 | 99.40 | 99.51 |
| Mg# | 61.1 | 62.9 | 58.6 | 57.6 | 61.5 |
| Modes (vol. %) | | | | | |
| Olivine | | | | | |
| ph | 2.4 | 1.6 | 1.2 | 1.0 | 2.8 |
| mph | 3.0 | 1.6 | 2.2 | 1.6 | 3.6 |
| Clinopyroxene | | | | | |
| ph | 0.8 | 0.8 | 0.4 | 0.8 | 1.0 |
| mph | 1.2 | 0.6 | 1.2 | 0.8 | 1.0 |
| Matrix | 92.6 | 93.2 | 95.0 | 95.8 | 91.6 |
| Vesicularity | 15–20 | 5 | 10–15 | 5–10 | 10–15 |

better understand their crystallization histories. The methods used in these analyses are the same as described in Garcia et al. (1995). The analyses reported in Table 2 are an average of three points/grain. The olivines form two compositionally distinct groups: one with higher forsterite contents (~87%) that includes re-sorbed and euhedral crystals, and the other with lower forsterite contents (81–82%) for euhedral crystals and inclusions in clinopyroxenes. All of the olivines are normally zoned, except the inclusions, which are unzoned. The clinopyroxenes are normally zoned in their cores away from the olivine inclusions but are reversely zoned near their rims (outer 0.01–0.02 mm; Table 2). The Al₂O₃ content of the clinopyroxene cores is higher than the rims (20–120% relative), which may indicate polybaric crystallization (e.g., Gasparik and Lindsley 1980).

Whole-rock and glass geochemistry

Whole-rock XRF analyses were made of five representative rocks from the RR cruise (Table 1) using methods described in Rhodes et al. (1988). These rocks exhibit a substantial range in MgO concentration (8.2–10.3 wt.%). The difference in MgO concentrations between the two glassy lavas (286-1 and 286-6) can be related to their modal differences in mafic minerals (~3 vol.%; Table 1). The Mg# [(Mg/Mg + Fe²⁺)x100] of the RR cruise lavas are relatively high for Hawaiian shield lavas (58–63; Table 1) indicating that they probably were not stored in the crust for significant time pe-

riods, which would have allowed crystallization of Mg-rich minerals

Glass was separated from each of the lava blocks collected during the RR cruise. It was then crushed, sieved, washed, and carefully picked using a binocular microscope for determination of major elements by electron microprobe, trace elements by laser ablation ICP-MS, volatiles by high-temperature Knudsen cell mass spectrometry, He isotopes by mass spectrometry, ²¹⁰Po analyses by α spectrometry, and Pb, Sr, Th, and U abundances and Pb, Sr, and Nd isotopic compositions by thermal ionization mass spectrometry. Major and trace element analyses were also determined for glasses from five pillow lavas collected from the Pisces Peak area (triangles in Fig. 1) during Alvin dive 1802 during 1987 (see Garcia et al. 1993 for more information on this dive).

The microprobe glass analyses are an average of five spot analyses on at least two grains per sample (see Garcia et al. 1995 for methods used). All of the breccia glasses are similar in composition to each other and to dive 1802 glasses, although there are subtle differences between the glasses (see Table 3). Like the vast majority of recent Loihi lavas (Garcia et al. 1995), the breccia glasses are low-SiO₂ tholeiites (Fig. 2). The MgO variation of the breccia glasses is limited (6.7–7.0 wt.%), which is probably an indication that the lavas were quenched at similar temperatures, ~1150 °C, based on the MgO thermometer for Kilauea tholeiites (Helz and Thornber 1987). This temperature is typical of the eruption temperature of the lavas from the ongoing Pu'u 'O'o eruption of Kilauea (e.g., Mangan et al.

Table 2 Representative microprobe analyses of the cores of olivines and the cores and rims of clinopyroxenes phenocrysts in lavas from Loihi 1996 eruption breccia. All values are in wt. % ex-

cept forsterite (Fo) and Mg# [$\text{Mg}/(\text{Mg} + \text{Fe}) \times 100$]. Olivine phenocrysts (ph), a resorbed phenocryst (rph), microphenocrysts (mph) and inclusions in clinopyroxene (incl) were analyzed

| | Olivine | | | | | | | |
|------------------|---------|--------|--------|--------|--------|-------|--------|-------|
| | 286-2 | | | | 286-6 | | | |
| | rph | ph | mph | incl | ph | ph | mph | incl |
| SiO ₂ | 40.25 | 39.3 | 39.2 | 39.15 | 40.1 | 39.2 | 39.1 | 38.9 |
| FeO | 12.0 | 17.05 | 17.0 | 17.24 | 12.25 | 16.9 | 17.4 | 17.9 |
| MnO | 0.16 | 0.23 | 0.22 | 0.25 | 0.18 | 0.25 | 0.24 | 0.24 |
| MgO | 47.3 | 43.1 | 43.3 | 42.8 | 47.2 | 43.2 | 43.0 | 42.25 |
| CaO | 0.28 | 0.32 | 0.31 | 0.36 | 0.29 | 0.36 | 0.36 | 0.38 |
| Total | 99.99 | 100.00 | 100.03 | 100.20 | 100.02 | 99.91 | 100.10 | 99.67 |
| Fo% | 87.5 | 81.8 | 82.0 | 81.6 | 87.3 | 82.0 | 81.5 | 80.0 |

| | Clinopyroxene | | | | | | | |
|--------------------------------|---------------|-------|-------|--------|-------|-------|-------|-------|
| | 286-2 | | | | 286-6 | | | |
| | Core | Rim | Core | Rim | Core | Rim | Core | Rim |
| SiO ₂ | 49.7 | 50.95 | 49.25 | 51.2 | 49.85 | 51.0 | 48.6 | 52.0 |
| TiO ₂ | 1.20 | 0.76 | 1.35 | 0.78 | 1.16 | 0.96 | 1.4 | 0.78 |
| Al ₂ O ₃ | 4.25 | 2.78 | 4.55 | 2.95 | 4.15 | 3.4 | 5.1 | 2.3 |
| Cr ₂ O ₃ | 0.80 | 0.78 | 0.87 | 0.82 | 0.82 | 0.62 | 0.95 | 0.57 |
| FeO | 6.30 | 5.55 | 6.35 | 5.60 | 6.10 | 5.59 | 6.8 | 5.70 |
| MnO | 0.12 | 0.11 | 0.13 | 0.12 | 0.12 | 0.14 | 0.15 | 0.13 |
| MgO | 15.5 | 16.45 | 15.3 | 16.8 | 15.65 | 16.25 | 15.3 | 16.95 |
| CaO | 21.5 | 21.5 | 21.5 | 21.6 | 21.6 | 21.3 | 20.6 | 21.0 |
| Na ₂ O | 0.26 | 0.25 | 0.28 | 0.25 | 0.25 | 0.25 | 0.28 | 0.22 |
| Total | 99.63 | 99.13 | 99.58 | 100.12 | 99.70 | 99.87 | 99.18 | 99.65 |
| Mg# | 81.5 | 84.1 | 81.1 | 84.2 | 82.0 | 83.0 | 80.0 | 84.1 |

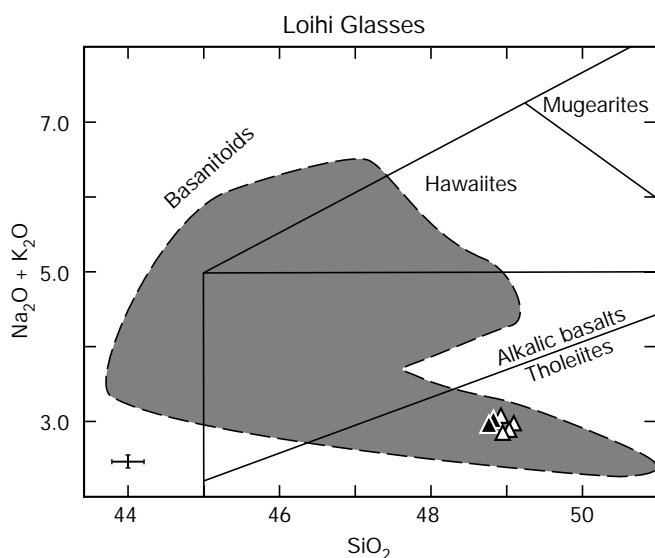


Fig. 2 SiO₂ vs total alkalis (Na₂O + K₂O) plot for Loihi glasses (all values in weight percent). The dashed line encompasses the stippled field for all Loihi glasses (see Garcia et al. 1995). The field boundaries for rock compositions are from LeBas et al. (1986), except the dividing line for tholeiites and alkalic basalts, which is from Macdonald and Katsura (1964). Closed triangles 1996 eruption lavas; open triangles other blocks from the 1996 breccia. Note that the glasses from the 1996 breccia are all tholeiitic and occupy only a small portion of the Loihi field. Two-sigma error bars are given in the lower left corner

1995). The CaO contents of these Loihi glasses are high compared with typical Hawaiian tholeiites (~12.0 vs. 10–11 wt.%), which may explain the presence of clinopyroxene in these relatively mafic tholeiites. Typically, Hawaiian tholeiites with MgO > 6.8 wt.% contain only olivine (e.g., Wright 1971; Garcia et al. 1996). The slightly variable CaO/Al₂O₃ ratios at nearly the same MgO in these glasses (0.85–0.89; Fig. 3) is probably the result of minor clinopyroxene fractionation, which occurs as both phenocrysts and microphenocrysts in these rocks (Table 1). One sample has distinctly lower TiO₂ (Fig. 3) and, therefore, must have a different parental magma from the other lavas.

Volatile concentrations (H₂O, S, Cl, and CO₂) were determined for the glasses from the two fresh Loihi lavas (Table 3) and one “older” breccia sample using techniques described by Byers et al. (1985). The H₂O concentration in these glasses (~0.60 wt.%) are among the highest values reported for Loihi tholeiitic pillow rim glasses (0.35–0.61 wt.%; Byers et al. 1985; Garcia et al. 1989). The CO₂ and Cl concentrations for these glasses are on the low side of the range of previous values (CO₂– 0.035–0.046 vs 0.03–0.17 wt.%; Cl– ~0.07 vs 0.06–0.11 wt.%; S concentrations in the glasses (~0.11 wt.%) are well within the range of other Loihi tholeiitic glasses (0.08–0.17 wt.%).

Trace element analyses were performed on glasses from six RR cruise rocks and five pillow lavas from the

Table 3 Major element, volatile, and helium isotope analyses of glass from the Loihi 1996 eruption breccia and from lavas collected along the northwest rim of Loihi's west pit during ALVIN dive 1802 in 1987. Major elements were determined using a mi-

croprobe; volatiles by high-temperature Kundersen cell mass spectrometry; He isotopes by mass spectrometry (see text). All values are in wt. % except as noted. Total iron reported as FeO*

| Sample | 286-1 | 286-2 | 286-4 | 286-5 | 286-6 | 287-1 | 1802-22 | 1802-24 | 1802-25 |
|--|---------------------|-------|-------|--------------------|--------|-------|---------|---------|---------|
| Major elements | | | | | | | | | |
| SiO ₂ | 48.75 | 49.0 | 48.85 | 48.95 | 48.9 | 49.1 | 49.2 | 49.4 | 49.3 |
| TiO ₂ | 2.63 | 2.56 | 2.62 | 2.64 | 2.68 | 2.62 | 2.61 | 2.73 | 2.67 |
| Al ₂ O ₃ | 13.7 | 13.8 | 13.6 | 13.9 | 13.8 | 13.8 | 13.71 | 13.85 | 13.8 |
| FeO* | 11.8 | 11.5 | 11.6 | 11.9 | 11.8 | 11.9 | 12.0 | 11.7 | 11.6 |
| MnO | 0.14 | 0.16 | 0.15 | 0.15 | 0.15 | 0.16 | 0.18 | 0.19 | 0.17 |
| MgO | 6.91 | 6.85 | 7.01 | 6.80 | 6.72 | 6.85 | 6.80 | 6.73 | 6.87 |
| CaO | 12.05 | 11.75 | 12.15 | 12.1 | 11.95 | 11.95 | 11.72 | 11.8 | 11.8 |
| Na ₂ O | 2.53 | 2.48 | 2.60 | 2.60 | 2.56 | 2.52 | 2.48 | 2.49 | 2.49 |
| K ₂ O | 0.45 | 0.39 | 0.43 | 0.44 | 0.46 | 0.40 | 0.42 | 0.43 | 0.41 |
| P ₂ O ₅ | 0.24 | 0.20 | 0.21 | 0.22 | 0.24 | 0.20 | 0.27 | 0.25 | 0.24 |
| Total | 99.20 | 98.65 | 99.21 | 99.70 | 99.28 | 99.52 | 99.39 | 99.66 | 99.66 |
| Volatiles | | | | | | | | | |
| H ₂ O | 0.625 | | | 0.586 | 0.606 | | | | |
| CO ₂ | 0.035 | | | 0.046 | 0.041 | | | | |
| S | 0.108 | | | 0.116 | 0.103 | | | | |
| Cl | 0.072 | | | 0.073 | 0.069 | | | | |
| Subtotal | 0.840 | | | 0.821 | 0.819 | | | | |
| Total | 100.04 | | | 100.52 | 100.00 | | | | |
| Helium and vesicle CO₂ | | | | | | | | | |
| <i>Crushed (vesicle)</i> | | | | | | | | | |
| ³ He/ ⁴ He | 25.0 ± 0.3 | | | 24.8 ± 0.2 | | | | | |
| He, ncc/g | 12.43 | | | 34.45 | | | | | |
| CO ₂ , cc/g | 0.000100 | | | 0.000687 | | | | | |
| C/ ³ He | 2.32E+08 ± 5.0E+0.7 | | | 5.79E+08 ± 4.4E+07 | | | | | |
| C/ ⁴ He | 8.07E+03 | | | 1.99+04 | | | | | |
| <i>Melted powder</i> | | | | | | | | | |
| ³ He/ ⁴ He | 25.0 ± 0.3 | | | 24.4 ± 0.4 | | | | | |
| He, ncc/g | 48.74 | | | 44.41 | | | | | |

Alvin dive 1802 using the laser ablation ICP-MS technique (Table 4; see Norman et al. 1996 for a description of the methods used). Two samples (286-1, 287-1) were analyzed twice using separate splits; the replicate values agree to within 1% for all elements except Ni and Ho at 1–2%, and Eu, U, and Lu at ~3% (Table 4).

The concentrations of trace elements in these glasses are typical of those for Loihi tholeiites (see Garcia et al. 1995). For example, the REE patterns for the breccia glasses are similar to those for Loihi tholeiites, including a slightly positive Eu anomaly. The slopes of the REE patterns for the breccia samples are slightly flatter than for most Loihi tholeiites, which is reflected in their slightly lower La/Yb ratios (5.2–5.7 vs 5.6–7.5; Fig. 4). The glasses from the surface flows in the Pisces Peak area collected in 1987 during Alvin dive 1802 have similar low La/Yb ratios (5.1–5.3; Fig. 4).

Sr, Nd, and Pb concentrations and isotopic ratios were determined for the glassy breccia samples using methods described by Mahoney et al. 1991 (Table 5). The Sr and Pb isotopic ratios for the two samples are remarkably similar to each other (within analytical error) and are typical of values obtained for other Loihi lavas, especially recent summit lavas (Fig. 5).

Th and U abundances were determined by thermal ionization mass spectrometry (TIMS) in the two glassy lavas using ²²⁹Th and ²³³U spikes (Table 5). The accuracy of our concentration measurements was verified by analyses of three rock standards (BHVO-1, BCR-1, and JB-1a), all of which agree to within 1.5%. Although the TIMS U and Th data are slightly lower than the laser-determined values, the two data sets are within 2-σ errors. The concentrations of Th and U in the glasses from these two lavas are similar to those of Kilauea tholeiites (see Jochum and Hofmann 1995), but the Th/U for Loihi are slightly higher (3.2 vs 3.0 ± 0.1).

³He/⁴He ratios were determined both by crushing and by melting powders from the crushing experiments (dissolved component) on two 1996 breccia samples (286-1 and 286-5), following methods outlined in Graham et al. (in press). The ³He/⁴He ratios for both samples by each method are nearly identical within analytical uncertainty (sample 286-5 had a slightly lower dissolved ³He/⁴He) and all values are ~25 times the atmospheric ratio (R_A; Table 3). Intriguingly, each sample also has the same amount of “dissolved” helium (released by fusion; 47.3 ± 3.0 × 10⁻⁹ STP/g), although they differ in their vesicle helium contents by a factor

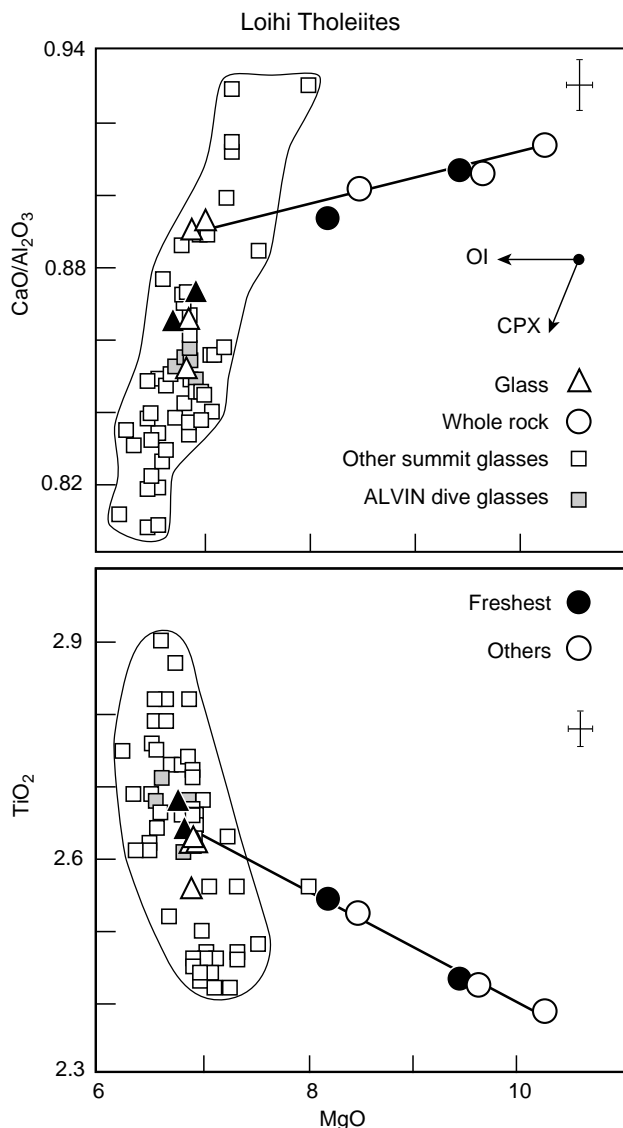


Fig. 3 MgO variation diagrams of TiO_2 and $\text{CaO}/\text{Al}_2\text{O}_3$ for Loihi summit tholeiites. Symbols as in Fig. 2, except closed circles for whole rocks from the 1996 eruption; open circles for other whole rocks from the 1996 breccia; shaded squares for the prehistoric Alvin dive 1802, samples 20–25 glasses, and open squares for other Loihi summit tholeiite glasses (data from Garcia et al. 1993, 1995). The range in $\text{CaO}/\text{Al}_2\text{O}_3$ among the 1996 breccia glasses probably represents variable amounts of clinopyroxene crystallization from similar parental magmas. Arrows show the expected effects of olivine-only (OI) and clinopyroxene (CPX) fractionation. The whole-rock compositions and most of the glasses are colinear for TiO_2 which is probably caused by magma mixing. Note the wide TiO_2 range for other Loihi tholeiites but the relatively restricted range for glasses from the 1996 breccia and the Alvin 1802 lavas. Two-sigma error bars are given in the upper right portion of each plot

of 3 (released by crushing; 12 vs 35×10^{-9} STP/g in 286-1 and 286-5, respectively). The factor of 3 difference in vesicle helium content may be due to differences in vesicle sorting within the magma during ascent or to bubble loss during eruption. The vesicle $\text{CO}_2/{}^3\text{He}$ ratios

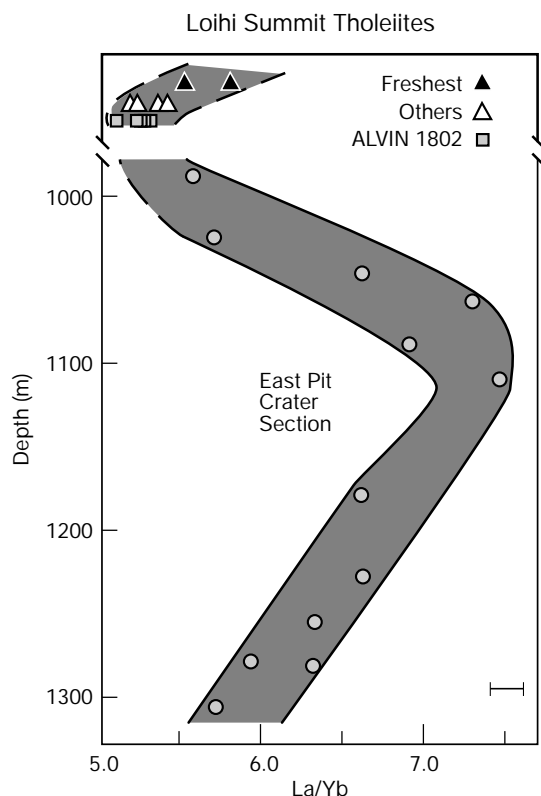


Fig. 4 Variation in the La/Yb ratios with stratigraphic position for tholeiitic glasses from Loihi's east pit crater (gray circles; only more mafic samples, >6.7 wt.% MgO , are shown to avoid the effects of crystal fractionation; Garcia et al. 1993), from Alvin dive 1802 samples 20–25 and from the 1996 breccia (symbols as in Fig. 3). Note the break in section between the east pit section and surface samples from the Pisces Peak area, the shallowest feature on Loihi. The temporal variation that was noted for the east pit samples (stippled band) seems to continue for the Alvin samples and the older 1996 breccia samples but may have reversed for the 1996 eruption glasses. A 2- σ error bar is given in the lower right corner of the plot for the new analyses

measured in samples 286-1 and 286-5 were 2.3 and 5.8×10^8 (Table 3).

The ${}^3\text{He}/{}^4\text{He}$ ratios of the two 1996 breccia samples (24.8–25.0 R_A) are within the range reported previously for Loihi seamount (20–32 R_A ; Kurz et al. 1983; Rison and Craig 1983; Kaneoka et al. 1983; Hiyagon et al. 1992; Honda et al. 1993). The new ${}^3\text{He}/{}^4\text{He}$ ratios are higher than the ratio of 22.5 R_A measured for an evolved alkali basalt glass previously sampled from the nearby Pele's vents area in 1987 (1804-19; D. W. Graham, unpublished data).

Geochronology

Eruption ages for the two freshest Loihi breccia samples (286-1 and 286-6) have been determined using the ${}^{210}\text{Po}$ – ${}^{210}\text{Pb}$ method (Rubin et al. 1994). This technique relies upon the fact that ${}^{210}\text{Po}$ is volatile at magmatic temperatures (Vilenskiy 1978; Le Guern et al. 1982)

Table 4 Laser ablation ICP-MS analyses of trace elements in glasses from the Loihi 1996 eruption breccia and lavas from the Pisces Peak area collected in 1987. Samples 286-1 and 287-1 were

analyzed twice and the values are averaged. All values are in ppm

| Sample | 1996 Eruption breccia | | | | | | Prehistoric Pisces Peak area | | | | |
|--------|-----------------------|-------|-------|-------|-------|-------------|------------------------------|---------|---------|---------|---------|
| | 286-1 | 286-2 | 286-4 | 286-5 | 286-6 | 287-1 | 1802-20 | 1802-22 | 1802-23 | 1802-24 | 1802-25 |
| Cs | 0.10 | — | 0.10 | 0.09 | 0.10 | 0.11 | 0.07 | 0.09 | 0.09 | 0.10 | 0.07 |
| Rb | 9.9 ± 0.1 | 9.0 | 10.1 | 9.55 | 10.0 | 9.0 ± 0.1 | 8.1 | 8.8 | 9.0 | 10.0 | 8.8 |
| Ba | 121 ± 1 | 114 | 130 | 126 | 127 | 117 ± 1 | 112 | 111 | 113 | 121 | 112 |
| Nb | 15.9 ± 0.1 | 15.9 | 17.2 | 16.8 | 16.9 | 16.1 ± 0.2 | 15.9 | 15.5 | 15.8 | 16.8 | 15.4 |
| Ta | 0.95 ± 0.01 | 0.98 | 1.00 | 1.01 | 1.03 | 0.98 ± 0.00 | 0.99 | 0.92 | 0.94 | 0.98 | 0.95 |
| U | 0.29 ± 0.01 | 0.26 | 0.34 | 0.29 | 0.31 | 0.28 ± 0.01 | 0.28 | 0.28 | 0.29 | 0.32 | 0.29 |
| Th | 0.87 ± 0.01 | 0.88 | 0.97 | 0.92 | 0.95 | 0.92 ± 0.01 | 0.87 | 0.81 | 0.84 | 0.90 | 0.84 |
| Pb | 1.6 ± 0.2 | 1.5 | 1.4 | 1.5 | 1.6 | 1.4 ± 0.0 | 1.3 | 1.3 | 1.3 | 1.5 | 1.5 |
| La | 12.6 ± 0.1 | 12.5 | 13.3 | 12.8 | 13.1 | 12.3 ± 0.1 | 12.1 | 11.6 | 12.0 | 12.7 | 12.0 |
| Ce | 30.5 ± 0.2 | 29.9 | 32.6 | 31.2 | 31.8 | 30.0 ± 0.3 | 29.5 | 29.2 | 29.7 | 31.9 | 29.5 |
| Pr | 4.52 ± 0.03 | 4.53 | 4.82 | 4.64 | 4.76 | 4.55 ± 0.01 | 4.38 | 4.38 | 4.43 | 4.61 | 4.42 |
| Nd | 21.4 ± 0.01 | 21.8 | 23.0 | 21.8 | 22.4 | 21.8 ± 0.0 | 20.9 | 2.02 | 20.7 | 22.5 | 21.0 |
| Sm | 5.57 ± 0.03 | 5.87 | 5.59 | 5.50 | 5.66 | 5.53 ± 0.25 | 5.31 | 5.26 | 5.41 | 5.73 | 5.45 |
| Eu | 1.87 ± 0.01 | 1.95 | 2.04 | 1.87 | 1.91 | 1.85 ± 0.05 | 1.92 | 1.83 | 1.86 | 1.96 | 1.84 |
| Gd | 5.70 ± 0.01 | 5.72 | 5.87 | 5.94 | 6.00 | 5.95 ± 0.04 | 5.70 | 5.45 | 5.57 | 5.98 | 5.81 |
| Dy | 5.3 ± 0.1 | 5.8 | 5.35 | 5.35 | 5.55 | 5.6 ± 0.0 | 5.29 | 5.13 | 5.18 | 5.57 | 5.70 |
| Ho | 1.02 ± 0.02 | 1.07 | 1.02 | 1.07 | 1.06 | 1.12 ± 0.01 | 1.06 | 0.99 | 0.99 | 1.05 | 1.05 |
| Er | 2.51 ± 0.02 | 2.82 | 2.84 | 2.72 | 2.82 | 2.78 ± 0.02 | 2.65 | 2.62 | 2.58 | 2.88 | 2.73 |
| Yb | 2.27 ± 0.02 | 2.38 | 2.45 | 2.45 | 2.28 | 2.28 ± 0.01 | 2.28 | 2.21 | 2.26 | 2.42 | 2.35 |
| Lu | 0.31 ± 0.01 | 0.32 | 0.33 | 0.32 | 0.34 | 0.33 ± 0.01 | 0.33 | 0.30 | 0.31 | 0.34 | 0.32 |
| Sr | 381 ± 1 | 372 | 397 | 394 | 398 | 378 ± 3 | 369 | 360 | 367 | 387 | 369 |
| Zr | 146 ± 1 | 154 | 157 | 155 | 154 | 154 ± 0 | 146 | 139 | 143 | 154 | 147 |
| Hf | 3.70 ± 0.05 | 3.92 | 3.92 | 3.88 | 3.99 | 3.39 ± 0.07 | 3.91 | 3.61 | 3.63 | 4.05 | 3.94 |
| Y | 26.2 ± 0.1 | 27.3 | 26.7 | 27.4 | 27.3 | 27.7 ± 0.1 | 26.3 | 25.1 | 25.6 | 27.6 | 26.6 |
| Sc | 33.3 ± 0.1 | 33.4 | 34.0 | 33.5 | 32.6 | 33.6 ± 0.1 | 32.0 | 31.6 | 31.3 | 32.0 | 33.0 |
| V | 378 ± 2 | 371 | 386 | 380 | 387 | 384 ± 2 | 377 | 383 | 384 | 414 | 376 |
| Co | 47.5 ± 1 | 48 | 48 | 45 | 46 | 47 ± 0 | 45 | 46 | 47 | 51 | 47 |
| Ni | 92 ± 2 | 90 | 97 | 84 | 82 | 85 ± 1 | 83 | 87 | 84 | 87 | 87 |

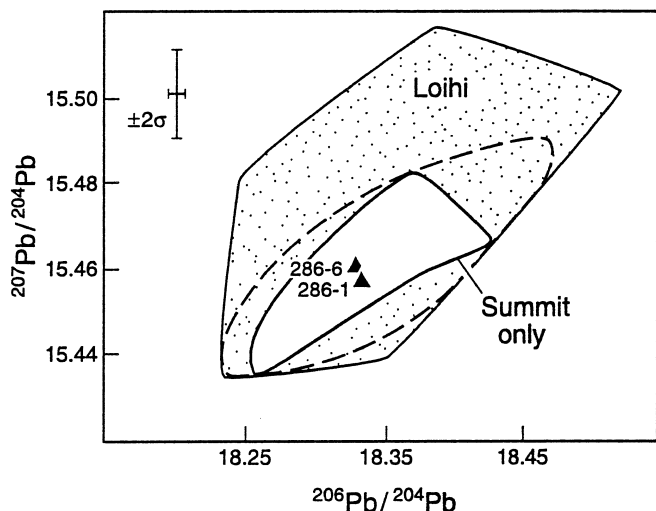


Fig. 5 Pb isotopic ratio plot for Loihi lavas. The large field encompasses all published Loihi data (~30 analyses; see Garcia et al. 1995 for data sources); the intermediate-size elongate field (bounded by the dashed line) is only for data from the University of Hawaii isotope lab (16 analyses); the smaller field is for just summit samples determined at the University of Hawaii (eight analyses), which are probably among Loihi's youngest lavas (Garcia et al. 1993). The two new 1996 breccia samples are nearly identical to each other in their Pb isotopic ratios and plot near the center of the summit field. Two-sigma error for these isotope ratios is shown in the upper left corner of the plot

and degasses nearly completely (95–100%) from erupting subaerial (Gill et al. 1985; Bennett et al. 1982) and shallow submarine basalts (Rubin and Macdougall 1989). In basalts erupted in >2-km-deep water, Po degassing has been observed to be 75% (Rubin et al. 1994). This degassing during eruption starts a “clock” within the lava that results in a measurable radioactive disequilibrium between ^{210}Po and grandparental ^{210}Pb that persists for 2–2.5 years. An age is determined by repeatedly analyzing the activity of ^{210}Po in a lava over a few of its half lives ($t_{1/2} = 138.4$ days) and a fit of the resulting data to an exponential ingrowth curve for the ^{210}Po – ^{210}Pb pair. ^{210}Po is an α particle emitter in the ^{238}U decay scheme and was analyzed at the University of Hawaii by α spectrometry.

In this grandparent–granddaughter pair, time since eruption diminishes the magnitude of radioactive disequilibrium, generally equating to poorer age resolution on a given sample the longer the time between eruption and the first ^{210}Po analysis. For this reason, analyses were begun on two fresh 1996 eruption breccia glasses as soon as practical following sample collection (within ~2 months). Our analytical techniques are summarized in the legend for Fig. 6.

Sample ages were calculated by regressing the ^{210}Po time series data to the equation

$$(^{210}\text{Po})_t = (^{210}\text{Po})_{t=0} \times [e^{-\lambda t}] + (^{210}\text{Pb}) \times [1 - e^{-\lambda t}],$$

Table 5 Thermal ionization mass spectrometry data and alpha spectrometry ^{210}Pb data for the two fresh glasses from the Loihi 1996 eruption breccia. Elemental abundances are in ppm; activities, in parenthesis by convention, are in dpm/g

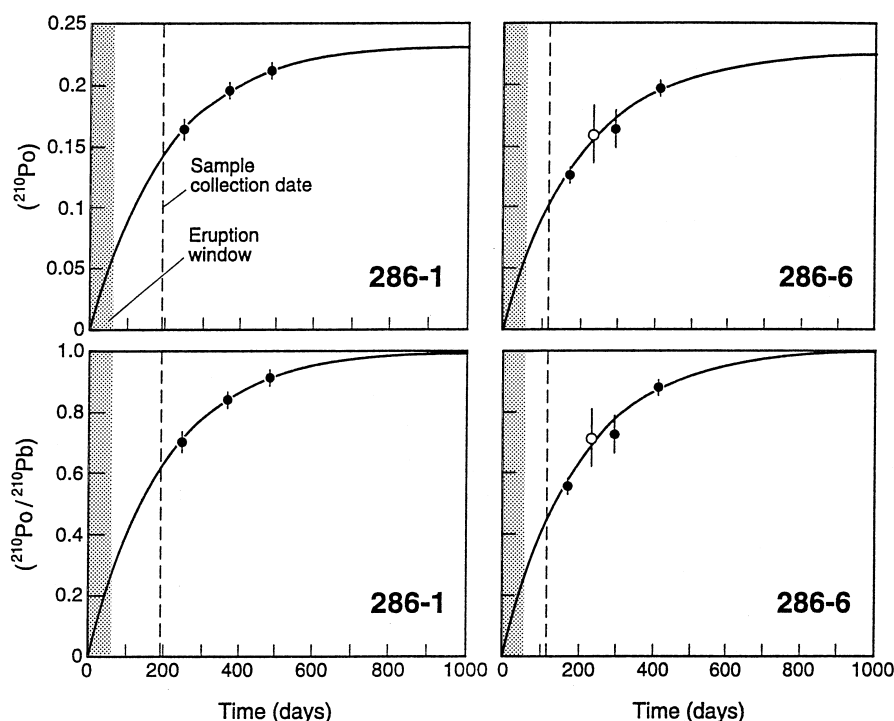
| Sample | 286-1 | 286-6 |
|------------------------------------|----------|----------|
| $^{206}\text{Pb}/^{204}\text{Pb}$ | 18.330 | 18.328 |
| $^{207}\text{Pb}/^{204}\text{Pb}$ | 15.457 | 15.460 |
| $^{208}\text{Pb}/^{204}\text{Pb}$ | 38.054 | 38.059 |
| $^{143}\text{Nd}/^{144}\text{Nd}$ | 0.512967 | — |
| $^{87}\text{Sr}/^{86}\text{Sr}$ | 0.703479 | 0.703466 |
| Pb | 1.15 | 1.13 |
| Nd | 20.76 | — |
| Sr | 372 | — |
| Th | 0.867 | 0.896 |
| U | 0.270 | 0.280 |
| Th/U | 3.211 | 3.203 |
| (^{210}Pb) | 0.232 | 0.225 |
| $(^{210}\text{Pb}/^{238}\text{U})$ | 1.16 | 1.09 |

All analyses were made at the University of Hawaii. Sr and Nd measurements were made using a VG Sector solid-source mass spectrometer; Pb, Th and U analyses were made on a VG Sector 54 fitted with a WARP filter. ^{210}Pb activities were derived from repeat ^{210}Po measurements (see Fig. 6 and text). Po measurements were made with partially depleted Si barrier detectors. Sr isotopic fractionation corrections are $^{86}\text{Sr}/^{88}\text{Sr}=0.1194$. The Sr and Nd isotopic data are reported relative to standard values for NBS 987, $^{87}\text{Sr}/^{86}\text{Sr}=0.710258$, and La Jolla Nd ($^{143}\text{Nd}/^{144}\text{Nd}=0.511855 \pm 0.000012$). Pb isotopic ratios are corrected for fractionation using the NBS 981 Pb standard values of Todt et al. (1984). The estimated uncertainties (2σ) are based on repeated measurements of the standards: $^{206}\text{Pb}/^{204}\text{Pb}$, ± 0.011 ; $^{207}\text{Pb}/^{204}\text{Pb}$, ± 0.010 , $^{208}\text{Pb}/^{204}\text{Pb}$, ± 0.024 ; $^{87}\text{Sr}/^{86}\text{Sr}$, ± 0.000024 . Within-run uncertainties on individual sample measurements of Pb and Sr isotopic ratios are $\leq 1\sigma$ mean external uncertainties of the NBS 987 and NBS 981 standards in all cases. Total procedural blanks are negligible: < 10 – 20 pg for Pb, < 20 pg for Nd, < 120 pg for Sr, 5 pg for U, 2 pg for Th, and 0.002 dpm for ^{210}Po

where t is time since eruption, λ is the decay constant, $0.005007 \text{ day}^{-1}$, and parentheses indicate activities. The equation describes the closed-system ^{210}Po content of a degassed lava as a function of time. This equation applies rigorously only to the time evolution of the ^{210}Po – ^{210}Pb pair after the first 25 days following eruption. This is the time period after which any eruption-induced disequilibrium between ^{210}Bi (the only intermediate nuclide between the two) and ^{210}Pb will have been erased by their return to secular equilibrium.

The ingrowth regressions (Fig. 6) were determined by finding the best value of time (t) that fit the data to

Fig. 6 ^{210}Po time-series data, analytical error, and ^{210}Po ingrowth curves for the two freshest Loihi breccia samples. Ingrowth curves were determined by regression (as described in the text). Curves for raw ^{210}Po activity (dpm/g) and the $^{210}\text{Po}/^{210}\text{Pb}$ activity ratio are plotted vs time for both samples. Also shown are the “eruption window” (gray area) and date of sample collection (dashed line) for both samples. Aliquots of ^{208}Po spiked “mother solutions” prepared from 0.5 g of dissolved sample were periodically removed and analyzed over the course of 9 months for ^{210}Po activity to generate these time-series data. Aliquots were 33, 21, 16, and 30% of the total for sample 286-6; and 28, 25, and 47% of the total for sample 286-1. Samples were digested with HF/HNO₃, dissolved in 3 N HCl, spiked with a calibrated ^{208}Po tracer, dried to a small volume to equilibrate and then redissolved into a stock sample solution consisting of 20–40 ml of 3 N HCl. Po was plated onto Ag disks for α spectrometric analysis (Flynn 1968). Detector backgrounds were measured prior to counting each sample. Sample count times ranged from 10 to 20 days. The ^{208}Po tracer we used also contains a fraction of ^{209}Po , which can have a small peak overlap with ^{208}Po during counting depending on the sample plate quality. The difference between the $^{209}\text{Po}/^{208}\text{Po}$ ratio in each sample and the known value was used for peak overlap corrections to yield a best ^{208}Po integral in a manner similar to that of Fler and Bacon (1984)



the ingrowth function, where t is the time in days between eruption (unknown) and the date of the first ^{210}Po analysis in the time series (known). Additional analyses in the time series are assigned time values of $t+x_1$, $t+x_2$... $t+x_n$, where n represents the number of analyses in the time series and x_i represents the (known) time interval between the first and each additional analysis. The regressions are based on three aliquot measurements on both of the samples. Sample 286-1 had a correlation coefficient of >0.999 for its regression. A fourth aliquot was analyzed for sample 286-6 (shown as an open circle in Fig. 6), but the datum is questionable due to a very poor polonium α spectrum that resulted from an inferior source plate, so it was not included. The difference in curve parameters between the 4-point vs the 3-point regressions is very small, resulting in an age difference of only 3 days (which is well within the other sources of error). However, removing this one data point resulted in an improved correlation coefficient (R^2) from 0.722 to 0.997. ^{210}Pb activity can be determined from these regressions from $(^{210}\text{Po})_{t=\infty}$, where ∞ was approximated as 10,000 days (>70 half-lives). Samples 286-1 and 286-6 have $(^{210}\text{Pb})=0.232$ and 0.225, respectively, which are the same within error (± 5 and 7%).

Using each data regression, the maximum age of the lava is determined from the value of t where the ingrowth function intercepts the origin ($t=0$ and $(^{210}\text{Po})_{t=0}=0$). This point represents complete Po degassing (e.g., the case of all subaerial and shallow submarine basalts). Higher values of t are not allowed, as this results in negative $(^{210}\text{Po})_{t=0}$ (implying greater than 100% Po loss on eruption). Lower values of t correspond to incomplete degassing of Po upon eruption. If Po was not completely degassed from a lava upon eruption, the time corresponding to the intercept of the ingrowth function overestimates the true lava age. It is possible that Po was not completely degassed during the Loihi eruption(s), which occurred under more than 10 bars hydrostatic pressure. Because of uncertainty in the extent of Po degassing during the eruption, lava ages are reported as eruption "windows," which are the most probable time of eruption between the calculated maximum and estimated minimum ages (Fig. 7).

The minimum age bound of this window is conservatively estimated at 57 days using observations made on basalts erupted at $9^\circ 50' \text{N}$ on the East Pacific Rise in 1991 and 1992. Two of the five samples from this locale were $\geq 75\%$ degassed during eruption, since $(^{210}\text{Po}/^{210}\text{Pb})=0.25$ in these lavas on the date of sample collection (the ultimate "minimum" age). In constructing their eruption windows, it was assumed that all five of these basalts had very similar initial ^{210}Po (Rubin et al. 1994), because all had very similar chemical compositions and were erupted at the same 2.5-km water depth (both factors which should largely govern Po degassing efficiency). Thus, all of these Rise lavas were constrained to lie within the part of the ingrowth curve between 100 and 75% ^{210}Po degassing (which is a time

^{210}Po - ^{210}Pb dating: Loihi seamount

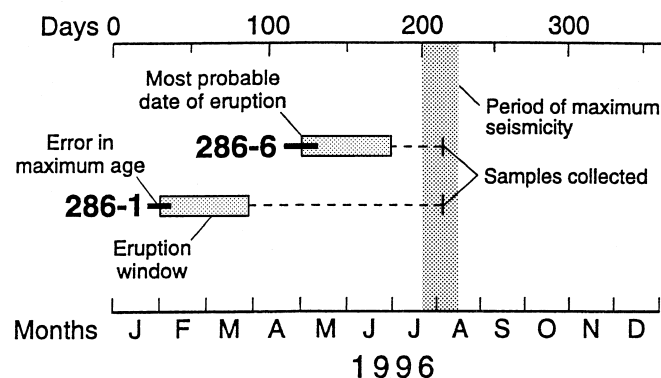


Fig. 7 "Eruption windows" (gray boxes) for Loihi 1996 glassy breccia lavas. These eruption windows are bounded by the dates of maximum (100%) and assumed minimum (75%; younger date) initial Po degassing (as discussed in the text). Also shown is the error in maximum age (black bars) based on data-regression quality, the date of sample collection, and the time period of the earthquake swarm (gray vertical band). These results indicate that the two glassy breccia lavas were erupted prior to the swarm, and have different eruption windows. Time scales are given in both days and months for reference

"window" of 57 days, or ~ 2 months). Although these are conservative time windows (as it is highly probable that the Rise lavas used to constrain the minimum age bound of the eruption windows were not erupted the day they were collected), we continue to use 2-month eruption windows for all submarine lavas erupted at depths >200 m until samples from deep eruptions can be confirmed to have degassed more than 75% of their Po upon eruption.

The eruption windows of samples 286-1 and 286-6 are from the first half of 1996, prior to the July to August earthquake swarm (Fig. 7). Sample 286-6 probably erupted in a 2-month interval starting 8 May ± 13 days, whereas sample 286-1 appears to have erupted during the 2-month interval starting on 28 January ± 7 days. The two eruption windows do not overlap even when analytical and regression errors are considered. The only scheme that would allow for these two lavas to have erupted together is for them to have been erupted in May with sample 286-1 to have degassed only 62% of its Po and the other lava to have degassed 100% of its Po. This variable degassing scheme for the two 1996 lavas is not supported by the other volatile data. Thus, it appears the ^{210}Po ages for the two very glassy lavas are distinct and predate the earthquake swarm. Unfortunately, we cannot narrow the width of the eruption windows using earthquake data because few earthquakes were recorded from the Loihi area during the first half of 1996. Loihi is monitored by the HVO seismic network, whose closest station is ~ 35 km from the summit of the volcano; thus, many Loihi earthquakes are unrecorded by the HVO network. This conclusion

is supported by data recorded by the ocean bottom seismograph that was located at the summit of Loihi and detected 471 Loihi earthquakes during the latter part of the 1996 earthquake swarm [during which time the HVO network detected only 23 (~5%) of the actual earthquakes; J. Caplan-Auerbach, pers. commun.].

How many Loihi eruptions in 1996?

In addition to the one or two dated eruptions during the first half of 1996, there is circumstantial evidence that an eruption was occurring on Loihi during the July–August 1996 earthquake swarm. Seawater sampled during the RR cruise from within the newly formed pit crater contained anomalously high ^{210}Po and other volatile heavy-metal concentrations (Rubin 1997), and anomalously high-temperature, pH and CO_2 signatures, and sonobuoys detected popping noises (Loihi Science Team 1997). All of these observations are consistent with an eruption at the summit of Loihi during the earthquake swarm. Whether there were three separate eruptions at Loihi within a 6-month period or just one prolonged eruption cannot be resolved with the current data.

Magmatic history of Loihi 1996 breccia blocks

The mineralogy of the blocks from the 1996 breccia records two distinct magmatic processes: magma mixing just prior to the eruption and moderate pressure crystal fractionation. A magma mixing event is indicated by the presence of reverse zoning in the clinopyroxene crystals and two compositionally distinct populations of olivine phenocrysts in the lava blocks. One of the magmas was mafic and contained only olivine with relatively high forsterite content (~87%). The other magma was more evolved and contained olivine with forsterite contents of 81–82% and clinopyroxene. The close proximity of reverse zoning to the clinopyroxene crystal margin (outer 0.01–0.02 mm) indicates that the mixing event probably occurred shortly before the eruption. How soon before eruption is unclear because we are unaware of any studies on the growth rates of clinopyroxene in basaltic liquids. If the rate for augite growth in a liquid of its own composition is used ($4 \times 10^{-5} \text{ cm s}^{-1}$; Dowty 1980), the mixing and eruption events would have been essentially simultaneous. This would indicate that mixing probably triggered the eruption.

An earlier magmatic history is recorded in the presence of olivine inclusions near the core of many clinopyroxene phenocrysts. Such inclusions are extremely rare in Hawaiian tholeiites because clinopyroxene is normally a late crystallizing phase (e.g., Wright 1971). To better understand the origin of these inclusions, the crystallization history of the fresh, more evolved 1996

MELTS Synthetic Phase Diagram

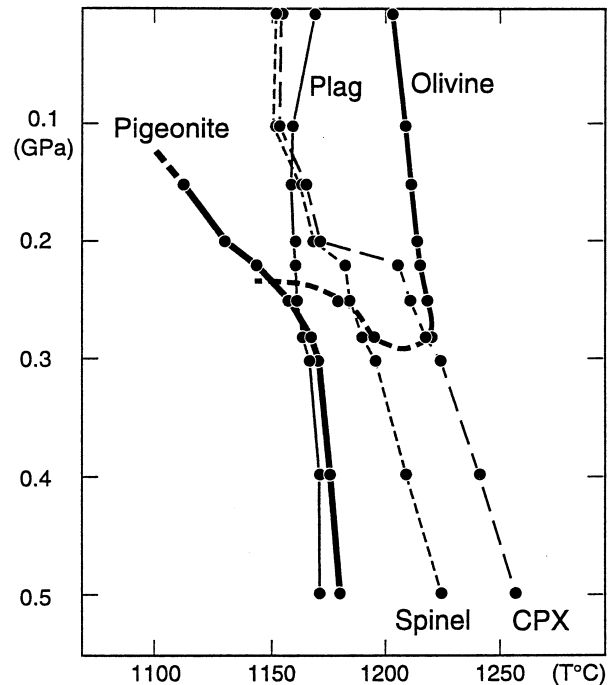


Fig. 8 Synthetic phase diagram created using the MELTS program (Ghiorso and Sack 1995) for the fresh, more evolved whole-rock composition (sample 286-6). Modeling conditions were 0.5 wt.% H_2O (the glass contained 0.61 wt.% H_2O), oxygen fugacity of 1 log unit below FMQ (based on the $\text{Fe}^{2+}/\text{Fe}^{3+}$ results of Byers et al. 1985), and equilibrium crystallization (i.e., crystals remained with the melt). For each pressure (shown by *dots*), the liquidus temperature was determined and then the magma was cooled in 1°C increments. The *dashed curve* for olivine marks its lower-temperature and higher-pressure stability limits

rock (286-6) was modeled using the MELTS program (Ghiorso and Sack 1995). The modeling was done at pressures ranging from 1 atm to 0.5 GPa under equilibrium crystallization conditions. The first step at each pressure was to find the liquidus temperature; the “magma” was then cooled in 1°C intervals and the proportion of each crystallizing phase was recorded (see Fig. 8 for the other modeling conditions).

The MELTS program indicates that olivine is the liquidus phase at pressures <0.3 GPa for the 8.2-wt.% MgO composition of sample 286-6. This result is consistent with the observation that olivine is the sole phenocryst in most Hawaiian tholeiites with MgO concentrations >7 wt.% MgO (e.g., Wright 1971; Garcia et al. 1996). At low pressures (0.1 GPa), olivine is followed by plagioclase and then clinopyroxene at temperatures $40\text{--}50^\circ\text{C}$ below the liquidus. For pressures of 0.22–0.28 GPa (depths of ~6.5–9 km), the temperature interval between the liquidus and the onset of clinopyroxene crystallization decreases to $<10^\circ\text{C}$. In this pressure interval, olivine reacts with the melt and is completely resorbed over a $\sim 30^\circ\text{C}$ temperature interval as clinopyroxene crystallizes; the dashed olivine curve in

Fig. 8 marks the temperature where olivine is completely resorbed by the cooling magma under equilibrium conditions. For pressures ≥ 0.3 GPa, olivine is no longer a stable liquidus phase and it is replaced by clinopyroxene (Fig. 8). This was an unexpected result because previous studies have assumed olivine is the liquidus phase at higher pressures (e.g., Wright 1971), although most experimental studies on Hawaiian tholeiitic compositions have used a more mafic starting composition (e.g., 16 wt.% MgO; Eggins 1992). However, unpublished experimental work by E. Tahakashi (pers. commun.) on Kilauea lava compositions found that olivine was stable only at low to moderate pressures for melts with 7.4–11 wt.% MgO.

The results from the MELTS modeling indicate that the magma for the 1996 breccia samples was stored at a pressure < 0.3 GPa to allow for the early crystallization of olivine, but at > 0.2 GPa to allow for crystallization of clinopyroxene without plagioclase. This moderate pressure is consistent with a pressure estimate of 0.37 to 0.39 ± 0.12 GPa at 1172 ± 15 °C for samples 286-2 and 286-6 determined from the clinopyroxene-melt thermobarometer of Putrika et al. (1996) using just the mineral core compositions, and the relatively high water and CO₂ concentrations in the glasses (Table 3). With this pressure constraint and assuming a normal mafic crust density of 2.85 g cm^{-3} for the region below the summit of Loihi (equal mixtures of oceanic crust layers 2 and 3; values from Kennett 1982), we estimated the probable depth of magma storage for the new Loihi lavas at 8–9 km (Fig. 9), which is ~ 1 km below the main concentration of earthquake hypocenters from the 1996 swarm (Loihi Science Team 1997). Magmatic earthquakes at Kilauea Volcano commonly occur just above magma bodies (e.g., Klein et al. 1987) and presumably the same is true for Loihi. Thus, the interpretations from the seismic and petrological modeling are in good agreement.

Our proposed magma chamber for the 1996 eruption (Fig. 9) is considerably deeper than a previous estimate for Loihi based on the neutral buoyancy model (2–3 km; Ryan 1987) and the inferred magma-chamber depths for the adjacent and more active Hawaiian volcanoes (i.e., Mauna Loa: 3–4 km depth; Decker et al. 1983; Kilauea: 3–6 km; Klein et al. 1987). However, it is much shallower than another depth estimate for a Loihi alkalic magma chamber (16 km; Clague 1988), which was based on CO₂ inclusions in ultramafic xenoliths from four Loihi alkalic lavas. The primary CO₂ inclusions in olivines from those xenoliths were reported to have been trapped at depths of 8–17 km (Roedder 1983). Our modeling does not preclude the existence of a deeper magma chamber at Loihi, especially during the previous alkalic stage. On the other hand, the CO₂ results for the Loihi ultramafic xenoliths do not require that their host lavas were stored at those depths. They only indicate that the host magmas probably were not stored in a shallower magma chamber after entraining the xenoliths. Furthermore, there is no mineralogical

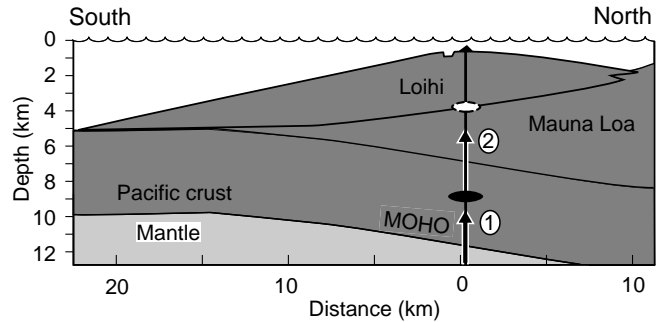


Fig. 9 Cross section of Loihi Volcano drawn to scale (no vertical exaggeration) showing the inferred basement for the volcano including lavas from Mauna Loa Volcano (probably interbedded with some Kilauea lavas), mid-Cretaceous (~ 105 Ma; Waggoner 1993) Pacific oceanic crust and mantle (see Garcia et al. 1995 for details on how the cross section was constructed). The intermediate depth (8–9 km) magma chamber for the 1996 and other recent Loihi tholeiitic eruptions is shown relative to the shallow level reservoir that was assumed to be present at Loihi (dashed oval). This is also the approximate depth within the volcano of the magma reservoir at the nearby active volcanoes, Mauna Loa and Kilauea (Decker et al. 1983; Klein et al. 1987), although those reservoirs may be considerably larger than the one shown. The location of the new Pele's pit crater is shown as a notch near the inferred vent location for the 1996 breccia. The first stage of the inferred magmatic history of this eruption (1) was the intrusion of mafic magma into the moderate depth reservoir, which contained more evolved magma. This mixing event is thought to have been rapidly followed by the eruption of this hybrid magma (2)

evidence for this deeper chamber (e.g., high-pressure pyroxenes) in Loihi lavas.

The longevity of our proposed 8- to 9-km-deep magma chamber was evaluated by an examination of the petrography of two suites of stratigraphically controlled Loihi lavas. One suite consists of three sections, each ~ 300 m deep, from the east and west summit pit craters (Fig. 1), and from along the crest of the upper portion of the south rift zone. These lavas are considered to be among the youngest on Loihi and are predominantly tholeiitic ($> 90\%$; Garcia et al. 1993). The other suite is from the deeply dissected east flank of Loihi; only the lavas from the upper few hundred meters of this section are tholeiitic. The rest of the section is dominantly alkalic ($\sim 90\%$; Garcia et al. 1995). Approximately 75% of the summit tholeiitic lavas contain clinopyroxene phenocrysts; 33% of these rocks have olivine inclusions in the clinopyroxenes, like the 1996 eruption blocks. In contrast, the east-flank lavas contain only phenocrysts of olivine; no clinopyroxene phenocrysts are present in any of the 35 samples from this section (Garcia et al. 1995). Thus, the older, predominantly alkalic lavas offer no record of the 8- to 9-km-deep magma reservoir, which is consistent with the interpretation of the CO₂ concentrations in the inclusions in the ultramafic xenoliths from Loihi alkalic lavas (Roedder 1983; Clague 1988).

Based on the mineralogical evidence presented above and the dominance of tholeiitic over alkalic lavas

among the youngest Loihi lavas (90–95%), we infer that the formation of a moderate-depth magma chamber is probably a recent occurrence related to the volcano's transition from alkalic to tholeiitic magmatism. This transition may have started at ~ 20 ka (Guillou et al. 1997) and may now be essentially complete. The formation of this magma chamber may be related to an increase in magma supply rate, which is thought to accompany the alkalic to tholeiitic transition on Hawaiian shield volcanoes (e.g., Frey et al. 1990). The greater depth of Loihi's magma chamber, compared with those at the more active shield volcanoes to the north, may be a consequence of Loihi's cooler thermal regime. Thus, the depth of Loihi's magma chamber may be controlled by thermal conditions, which are largely governed by magma supply rate, rather than by the volcano's density structure, as was proposed by Ryan (1987).

Temporal geochemical evolution of Loihi

A previous study of the geochemistry of lavas from a ~ 300 -m-thick stratigraphic section of tholeiites from Loihi's summit east pit crater showed a temporal variation in the ratios of highly to moderately incompatible elements (e.g., La/Yb; Garcia et al. 1993). Similar cyclic variations were noted for the Mauna Kea lavas from the Hawaii Scientific Drilling Project, where individual cycles may have spanned thousands of years (e.g., Yang et al. 1996), and for the historical lavas of Kilauea, where recent individual cycles may be only ~ 200 years long (1790–1982; A. Pietruszka and M. O. Garcia, unpublished data). In both cases, these trace element variations correlate with Pb and Sr isotopic variations indicating that this cyclicity is related to changes in proportions of the source components, which may be controlled by melting processes, and are modulated within a crustal magma chamber (A. Pietruszka and M. O. Garcia, unpublished data).

The older lavas from the 1996 eruption breccia and the surface lavas from the Pisces Peak area extend the temporal variation of Loihi summit tholeiites to lower values of La/Yb (Fig. 4). This trend appears to have reversed for the lavas from the 1996 eruption (Fig. 4). A reversal in the La/Yb ratio for historical Kilauea lavas is correlated with the collapse and accompanying explosions of the volcano's summit in 1924 (A. Pietruszka and M. O. Garcia, unpublished data). The La/Yb reversal at Loihi predates the 1996 earthquake swarm, but we cannot relate it to any specific volcanic or tectonic event at Loihi.

Pele's vents, previously most hydrothermally active locale on Loihi, is thought to be a site of recent volcanic activity (Garcia et al. 1993). An alkalic basalt collected from Pele's vents in 1987 (1804-19; Garcia et al. 1993) has the highest helium content yet measured for a Loihi basalt (4.5×10^{-6} ccSTP/g), a $\text{CO}_2/{}^3\text{He}$ ratio of 2.2×10^9 , and a vesicularity of 42 vol.%, indicating the gas-rich

nature of the Pele's vents magma. The 1996 breccia glasses are distinct from the Pele's vents glass in having mafic tholeiitic vs evolved alkalic compositions, relatively low ratios of vesicle $\text{CO}_2/{}^3\text{He}$, and distinct He isotope compositions (~ 25 vs $22.5 R_A$). These features clearly indicate that the 1996 breccia lavas were derived from a different magmatic source than the one which fed the very young alkalic lavas that formed Pele's vents.

The two glassy lavas from the 1996 breccia are remarkably similar in composition (see Tables 1, 2, 4, 5). The small differences that do exist can be explained by accumulation of ~ 3 vol.% olivine and clinopyroxene in sample 286-1. This implies that the two lavas were derived from the same magma reservoir, and that it changed little between the times the two lavas were erupted. The Alvin dive 1802 glasses from the Pisces Peak area are geochemically similar to the 1996 glasses, but ratios of highly over moderately incompatible elements are slightly lower for the Alvin samples (e.g., La/Yb; Fig. 4), indicating similar but distinct parental magmas for these lavas.

Do Loihi and Kilauea lavas have common parental magmas?

Seismically, the primary magma conduits for Loihi and Kilauea volcanoes appear to merge under the south flank of the island of Hawaii, and it has been proposed that they tap a common source (Klein 1982). Geochemically, tholeiites from Kilauea and Loihi tholeiites have strong isotopic, major and trace element similarities (Garcia et al. 1995). The small differences in SiO_2 and CaO concentrations between the lavas from these two volcanoes can be explained by high-pressure orthopyroxene fractionation in Loihi magmas (Garcia et al. 1995). To further examine how similar the magmas are from these two adjacent active volcanoes, we compared the incompatible trace element concentrations of the 1996 lavas and the other recent Loihi lavas to historical Kilauea summit lavas. A primitive mantle-normalized diagram with a linear scale, rather than the more commonly used log scale, was constructed for this comparison. The shape of the patterns for the Loihi breccia lavas are remarkably similar to those of the Alvin 1802 suite of samples, including negative anomalies for Th, U, Zr, and Hf, and a strong positive anomaly for Nb (Fig. 10). Thus, there appears to be a distinctive trace element geochemical signature among recent Loihi tholeiites.

Historical Kilauea summit lavas span the range of trace element ratios for this volcano and have Pb, Nd, and Sr isotopic ratios similar to the Loihi samples (A. Pietruszka and M. O. Garcia, unpublished data). The Kilauea lavas lack a strong positive Nb anomaly and have smaller negative Hf and Zr anomalies than do Loihi glasses (Fig. 10). The mild negative Sr anomaly in some Kilauea lavas (including the 1982 lava shown in

Fig. 10 Primitive mantle-normalized diagram comparing lavas from the Loihi 1996 eruption breccia, a representative sample from Alvin dive 1802, and the April 1982 Kilauea summit eruption. Note that the y-axis is plotted on a linear scale, rather than the commonly used log scale. The patterns for all of the Loihi samples are remarkably similar. In contrast, the Kilauea lava, like other historical Kilauea lavas, lacks a strong positive Nb anomaly and a steep drop between Nd and Zr. Mantle-normalizing values from Sun and McDonough (1989), except for Sr (23.4 ppm). Data sources: Table 4 for Loihi, and A. Pietruszka and M. O. Garcia (unpublished data) for Kilauea

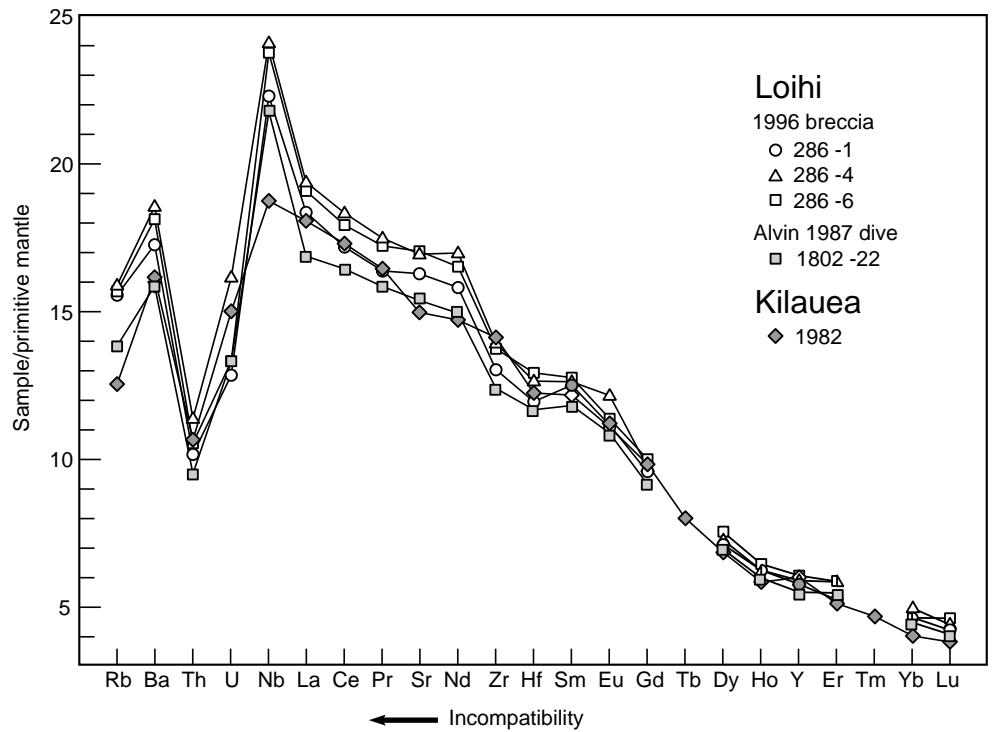


Fig. 10) is related to plagioclase fractionation (A. Pietruszka and M. O. Garcia, unpublished data). A common feature of these patterns is the nearly identical heavy REE and Y values for both the Loihi and Kilauea lavas, despite the slightly variable MgO contents of the lavas (7–10 wt.%; Fig. 10). Constant heavy REE and Y concentrations for fractionation-normalized lavas have been noted in many previous studies of Hawaiian lavas and explained by residual garnet in the source (e.g., Hofmann et al. 1984).

There are differences in the Th/U ratios of Loihi and Kilauea glasses that are not obvious in Fig. 10. All but 3 of the 45 published TIMS and spark source mass spectrometry analyses of Kilauea historical and prehistoric lavas have yielded Th/U ratios <3.05 and all are <3.15 (see Jochum and Hofmann 1995). In contrast, the two 1996 Loihi lavas have Th/U ratios of ~3.20 (TIMS data), and we have measured a ratio of 3.24 for an older alkalic Loihi lava. Even higher Th/U ratios (3.28–3.42) were reported by Sims et al. (1995) for three Loihi lavas. We conclude that although the sources for the Kilauea and Loihi lavas are similar isotopically and in trace elements, some important trace element differences are present. These differences indicate that magmas for Loihi and Kilauea do not share a common conduit at depth. Furthermore, the higher Th/U and Nb/La ratios for Loihi lavas might be related to a more primitive source (higher ratio) for Loihi lavas, which is consistent with He isotopic data for these lavas (e.g., Kurz et al. 1983).

Conclusion

Our petrological and geochronological results indicate that glassy Loihi lavas from a new breccia deposit were erupted in the first half of 1996, before the start of the July to August 1996 Loihi seismic event. The 1996 eruption(s) is the first documented historical eruption of Loihi, despite the ten earthquake swarms that have occurred at the volcano since 1970 and the numerous submersible dives and camera tow runs that have been made on the volcano. This eruption may have continued during the earthquake swarm based on the elevated water temperatures, anomalous geochemical features of water samples, and the popping noises recorded by sonobuoys during the swarm. The petrological and seismic evidence indicates that many of Loihi's tholeiitic magmas, including those from the 1996 eruption, were stored at moderate depths (~8–9 km). Mineralogical evidence indicates that some of these magmas were mixed with more mafic magmas shortly before eruption, which may have triggered their eruption. Loihi's moderately deep magma chamber is considerably deeper than the summit magma chambers for the other active Hawaiian volcanoes. This magma chamber may have developed during the past 10–20 ka as tholeiitic volcanism became dominant and the magma supply rate increased.

Acknowledgements Thanks to T. Kirby of the Hawaii Undersea Research Lab for his expert piloting of the PISCES V sub during the challenging conditions during the Loihi earthquake swarm and for other assistance, the Captain, crew, and the science team members from the Rapid Response cruise, especially the chief

scientist, F. Duennebieer. Thanks also to A. Sharma for assistance in the operation of the Macquarie University ICPMS, L. Sacks for help with the geochronological analyses, D. Macdougall of Scripps Institution of Oceanography for providing the calibrated ^{208}Po spike used in this study, J. Lupton for providing access to the NOAA helium mass spectrometer facility at the Hatfield Marine Science Center, J. Smith for the post-1996 earthquake swarm bathymetric base map of Loihi, A. Pietruszka for help with the MELTS program modeling, K. Putirka for help in using his CPX thermobarometer, M. Kramer for assistance with the UH α spectrometers and to D. Geist for helpful comments on a draft of this paper. This work was supported in part by grants from NSF to F. Duennebieer (OCE-9616913), which was approved expeditiously following the start of the earthquake swarm for a rapid response cruise, to K. Rubin (OCE-9633268) and D. Graham (OCE-9402506); and from the Australian Research Council and the Macquarie University to M. Norman. S. O'Reilly and the other members of GEMOC are thanked for their hospitality and assistance to M. Garcia during his sabbatical visit to Macquarie University. This paper is SOEST contribution #4632 and GEMOC publication #108.

References

- Bennett JT, Krishnaswami S, Turekian KK, Melson WG, Hupson CA (1982) The uranium and thorium decay series nucleides in Mt St Helens effusives. *Earth Planet Sci Lett* 60:61–69
- Bryan C, Cooper P (1995) Ocean bottom seismometer observations of seismic activity at Loihi Seamount, Hawaii. *Mar Geophys Res* 17:485–501
- Byers CD, Garcia MO, Muenow DW (1985) Volatiles in pillow rim glasses from Loihi and Kilauea volcanoes, Hawaii. *Geochim Cosmochim Acta* 49:1887–1896
- Caplan-Auerbach J, Duennebieer F, Okubo P (1997) Seismicity of the 1996 Loihi seamount eruption. *Geol Soc Am Abstr Prog* 29 (5): 7
- Clague DA (1988) Petrology of ultramafic xenoliths from Loihi seamount, Hawaii. *J Petrol* 29:1161–1186
- Decker RW, Koyanagi RY, Dvorak JJ, Lockwood JP, Okamura AT, Yamashita KM, Tanigawa WR (1983) Seismicity and surface deformation of Mauna Loa Volcano, Hawaii. *EOS* 64:545–547
- Dowty E (1980) Crystal growth and nucleation theory and the numerical simulation of igneous crystallization. *Physics of magmatic processes*. Princeton University Press, Princeton, pp 419–485
- Eggs SM (1992) Petrogenesis of Hawaiian tholeiites. 1. Phase equilibria constraints. *Contrib Mineral Petrol* 110:387–397
- Emery KO (1955) Submarine topography south of Hawaii. *Pacific Sci* 9:286–291
- Epp D (1984) Possible perturbations to hot spot traces and implications for the origin and structure of the Line Islands. *J Geophys Res* 89:273–286
- Fleer AP, Bacon MP (1984) Determination of ^{210}Pb and ^{210}Po in seawater and marine particulate matter. *Nucl Instr Meth Phys Res* 223:243–249
- Flynn WW (1968) The determination of low levels of polonium 210 in environmental materials. *Anal Chim Acta* 43:221–227
- Fornari DJ, Garcia MO, Tyce RC, Gallo D (1988) Morphology and structure of Loihi seamount based on Seabeam sonar mapping. *J Geophys Res* 93:15227–15238
- Frey FA, Wise WS, Garcia MO, West HB, Kwon S-T (1990) Evolution of Mauna Kea Volcano, Hawaii: petrologic and geochemical constraints on postshield volcanism. *J Geophys Res* 95:1271–1300
- Garcia MO, Muenow D, Aggrey K, O'Neil J (1989) Major element, volatile and stable isotope geochemistry of Hawaiian submarine tholeiitic glasses. *J Geophys Res* 94 (10): 525–538
- Garcia MO, Jorgenson B, Mahoney J, Ito E, Irving A (1993) An evaluation of temporal geochemical evolution of Loihi summit lavas. Results from Alvin submersible dives. *J Geophys Res* 98:537–550
- Garcia MO, Foss DJP, West WB, Mahoney JJ (1995) Geochemical and isotopic evolution of Loihi Volcano, Hawaii. *J Petrol* 26:1647–1674
- Garcia MO, Rhodes JM, Trusdell FA, Pietruszka A (1996) Petrology of lavas from the Puu Oo eruption of Kilauea Volcano. III. The Kupaianaha episode (1986–1992). *Bull Volcanol* 58:359–379
- Gasparik T, Lindsley DH (1980) Phase equilibria at high pressure of pyroxenes containing monovalent and trivalent ions. *Pyroxenes. Rev Mineral* 7:309–339
- Ghirosio MS, Sack RO (1995) Chemical mass transfer in magmatic systems IV. A revised and internally consistent thermodynamic model for the interpolation and extrapolation of liquid–solid equilibria in magmatic systems at elevated temperatures and pressures. *Contrib Mineral Petrol* 119:197–212
- Gill J, Williams R, Bruland K (1985) Eruption of basalt and andesite lava degasses ^{222}Rn and ^{210}Po . *Geophys Res Lett* 12:17–20
- Graham DW, Larsen LM, Hanan BB, Storey M, Pedersen AK, Lupton JE (in press) Helium isotope composition of the early Iceland mantle plume inferred from the Tertiary picrites of West Greenland. *Earth Planet Sci Lett*
- Guillou H, Garcia MO, Turpin L (1997) Unspiked K–Ar dating of young volcanic rocks from Loihi and Pitcairn hotspot seamounts. *J Volcanol Geotherm Res* 78:239–250
- Helz RT, Thornber CR (1987) Geothermometry of Kilauea Iki lava lake, Kilauea Volcano, Hawaii. *Bull Volcanol* 49:651–668
- Hiyagon H, Ozima M, Marty B, Zashu S, Sakai H (1992) Noble gases in submarine glasses from mid-ocean ridges and Loihi seamount: constraints on the early history of the Earth. *Geochim Cosmochim Acta* 56:1301–1316
- Hofmann AW, Feigenson MD, Raczek I (1984) Case studies on the origin of basalt. III. Petrogenesis of the Mauna Ulu eruption, Kilauea, 1969–1971. *Contrib Mineral Petrol* 88:24–35
- Honda M, McDougall I, Patterson DB, Dougeris A, Clague DA (1993) Noble gases in submarine pillow basalt glasses from Loihi and Kilauea, Hawaii: a solar component in the Earth. *Geochim Cosmochim Acta* 57:859–874
- Jochum KP, Hofmann AW (1995) Contrasting Th/U in historical Mauna Loa and Kilauea lavas. *Am Geophys Union Monogr* 92:307–314
- Kaneoka I, Takaoka N, Clague DA (1983) Noble gas systematics for coexisting glass and olivine crystals in basalts and dunite xenoliths from Loihi Seamount. *Earth Planet Sci Lett* 66:427–437
- Karl D, McMurtry G, Malahoff A, Garcia M (1988) Loihi Seamount: a midplate volcano with a distinctive hydrothermal system. *Nature* 335:532–535
- Kennett JP (1982) *Marine geology*. Prentice-Hall, New Jersey
- Klein FW (1982) Earthquakes at Loihi Submarine volcano and the Hawaiian hotspot. *J Geophys Res* 87:7719–7726
- Klein FW, Koyanagi RY, Nakata JS, Tanigawa WR (1987) The seismicity of Kilauea's magma system. *US Geol Surv Prof Pap* 1350:1019–1185
- Kurz MD, Jenkins WJ, Hart SR, Clague D (1983) Helium isotopic variations in the volcanic rocks from Loihi Seamount and the island of Hawaii. *Earth Planet Sci Lett* 66:388–406
- LeBas MJ, LeMaitre RW, Streckeisen A, Zanettin B (1986) A chemical classification of volcanic rocks based on the total alkalic–silica diagram. *J Petrol* 27:745–750
- Le Guern F, Le Rouley J–C, Lambert G (1982) Condensation du polonium dans les gaz volcaniques. *Acad Sci Paris Series II* 887:887–890
- Loihi Science Team (1997) Rapid response to submarine activity at Loihi Volcano, Hawaii. *EOS* 78:229–233

- Mahoney J, Nicollet C, Dupuy C (1991) Madagascar basalts: tracking oceanic and continental sources. *Earth Planet Sci Lett* 104:350–363
- Macdonald GA, Katsura T (1964) Chemical composition of the Hawaiian lavas. *Geol Soc Am Mem* 116:477–522
- Mangan MT, Heliker CC, Mattox TN, Kauahikaua JP, Helz RT (1995) Episode 49 of the Puu Oo-Kupaianaha eruption of Kilauea volcano: breakdown of a steady-state eruptive era. *Bull Volcanol* 57:127–135
- Moore JG, Clague DA, Normark WR (1982) Diverse basalt types from Loihi seamount, Hawaii. *Geology* 10:88–92
- Moore JG, Fiske RS (1969) Volcanic substructure inferred from the dredge samples and ocean-bottom photographs, Hawaii. *Geol Soc Am Bull* 80:1191–1202
- Norman MD, Person NJ, Sharma A, Griffin WE (1996) Quantitative analysis of trace elements in geological material by laser ablation ICPMS. *Geostandards Newslett* 20:247–261
- Putrika K, Johnson M, Kinzler R, Longhi J, Walker D (1996) Thermobarometry of mafic igneous rocks based on clinopyroxene-liquid equilibria, 0–30 kbar. *Contrib Mineral Petrol* 123:92–108
- Rhodes JM (1988) Geochemistry of the 1984 Mauna Loa eruption: implications for magma storage and supply. *J Geophys Res* 93:4453–4466
- Rison W, Craig H (1983) Helium isotopes and mantle volatiles in Loihi seamount and Hawaiian Island basalts and xenoliths. *Earth Planet Sci Lett* 66:407–426
- Roedder E (1983) Geobarometry of ultramafic xenoliths from Loihi seamount, Hawaii, on the basis of CO₂ inclusions in olivine. *Earth Planet Sci Lett* 66:369–379
- Rubin KH (1997) Degassing of metals and metalloids from erupting seamount and mid-ocean ridge volcanoes: Observations and prediction. *Geochim Cosmochim Acta* 61:3525–3542
- Rubin KH, Macdougall JD (1989) Submarine magma degassing and explosive magmatism at Macdonald (Tamarii) seamount. *Nature* 341:50–52
- Rubin KH, Macdougall JD, Perfit MR (1994) ²¹⁰Po–²¹⁰Pb dating of recent volcanic eruptions on the seafloor. *Nature* 368:841–844
- Ryan MP (1987) Neutral buoyancy and the mechanical evolution of magmatic systems. *Geochem Soc Spec Publ* 1:259–287
- Sims KWW, DePaolo DJ, Murrell MT, Baldrige WS, Goldstein SJ, Clague DA (1995) Mechanisms of magma generation beneath Hawaii and mid-ocean ridges: uranium/thorium and samarium/neodymium isotopic evidence. *Science* 267:508–512
- Sun S, McDonough WF (1989) Chemical and isotopic systematics of oceanic basalts: implications for mantle compositions and processes. *Geol Soc Lond*: 313–345
- Todt W, Cliff RA, Hanser A, Hofmann AW (1984) ²⁰²Pb + ²⁰⁵Pb double spike for lead isotopic analyses. *Terra Cogn* 4:209
- Vilenskiy VD (1978) Radium-226, lead-210 and polonium-210 in the products of the Tolbachik eruption in Kamchatka. *Geochim Int* 11:14–19
- Waggoner DG (1993) The age and alteration of central Pacific oceanic crust near Hawaii, site 843. *Proc Ocean Drilling Project Sci Results, Leg 136*:119–132
- Wright TL (1971) Chemistry of Kilauea and Mauna Loa lavas in space and time. *US Geol Surv Prof Pap* 735:1–45
- Yang H-J, Frey FA, Rhodes JM, Garcia MO (1996) Evolution of the Mauna Kea shield: inferences from lava compositions recovered in the Hawaii Scientific Drilling Project. *J Geophys Res* 101 (11): 747–768